

Nonlinear thermoelectricity with particle-hole symmetry in transport

G. Marchegiani,* A. Braggio,† and F. Giazotto‡

NEST Istituto Nanoscienze-CNR and Scuola Normale Superiore, I-56127 Pisa, Italy

(Dated: May 17, 2022)

In the linear regime, thermo-electric effects between two conductors are possible only in the presence of an explicit breaking of the electron-hole symmetry which results in the property $I(V) \neq -I(-V)$. We consider a tunnel junction between two electrodes and show that this condition is no longer required outside the linear regime. In particular, we demonstrate that a thermally-biased junction can display an absolute negative conductance (ANC), and hence thermo-electric power, at a small but finite voltage bias, provided that the density of states of one of the electrodes is gapped and the other is monotonically decreasing. We consider a prototype system that fulfills these requirements, namely a tunnel junction between two different superconductors where the Josephson contribution is suppressed. We discuss the main figures of merit of this nonlinear thermo-electric effect. We argue that the system may operate as an innovative thermo-electric memory and we predict that the setup can also sustain self-oscillations since, due to the ANC, it behaves as an active element at a low voltage bias.

Introduction. Recently, thermal transport at the nanoscale and the field of quantum thermodynamics have attracted a growing interest [1–8]. Researchers questioned whether classical thermodynamics is modified in the quantum regime and they discussed the effects on the performance of nanoscale heat engines [9–15]. In particular, thermo-electric systems have been extensively investigated [16–27], since they provide a direct thermal-to-electrical power conversion and could be exploited to save energy. In the linear regime, i.e. for a small voltage V and temperature bias ΔT , a necessary condition for thermoelectricity is breaking of electron-hole (EH) symmetry which results in the property $I(V) \neq -I(-V)$ [1], where I is the charge current flowing through the two terminal system. In fact, for $I(V, \Delta T) = -I(-V, \Delta T)$ it follows $I(0, \Delta T) = 0$ irrespectively of the temperature bias ΔT .

Here we question whether it is possible to have a finite thermo-electric power $\dot{W} = -IV > 0$ in a system characterized by EH symmetry in transport, by going beyond the linear regime. As we show below for a specific and universal case, the answer is positive.

Model. To answer the question, we consider a typical tunnel junction in the "semiconductor model" [28–30]: the system consists of two electrodes, here denoted with L, R, coupled through a thin insulating barrier where quantum tunneling takes place. We assume each electrode in internal thermal equilibrium, namely the quasiparticle distributions reads $f_\alpha(E - \mu_\alpha) = \{1 + \exp[(E - \mu_\alpha)/(k_B T_\alpha)]\}^{-1}$, where k_B is the Boltzmann constant and T_α, μ_α (with $\alpha = L, R$) are the temperatures and the chemical potentials of the quasiparticle systems, respectively. The quasiparticle charge and heat current flowing out of the α -electrode (with $\bar{\alpha} = R$ when $\alpha = L$ and *vice versa*) read [31]

$$\begin{pmatrix} I_\alpha \\ \dot{Q}_\alpha \end{pmatrix} = \frac{G_T}{e^2} \int_{-\infty}^{+\infty} dE \begin{pmatrix} -e \\ E \end{pmatrix} N_\alpha(E_\alpha) N_{\bar{\alpha}}(E_{\bar{\alpha}}) F_\alpha(E_\alpha) \quad (1)$$

where $-e$ is the electron charge, $N_\alpha(E)$ is the quasiparticle Density of states (DoS), $F_\alpha(E_\alpha) = f_\alpha(E_\alpha) - f_{\bar{\alpha}}(E_{\bar{\alpha}})$, $E_\alpha = E - \mu_\alpha$, and G_T is the conductance of the junction if both the electrodes have constant N_α . For simplicity, we assumed spin-degeneracy, and a energy and spin independent tunneling transmission matrix in the derivation of Eqs. 1. In the presence of a voltage bias V , the two chemical potentials are shifted with respect to each other, namely $\mu_L - \mu_R = -eV$. Below, we measure the energy E with respect to μ_L , i.e. we set $\mu_L = 0, \mu_R = eV$ and we define $I = I_L$ [32]. The expressions of Eqs. 1 satisfy the laws of thermodynamics [1, 22]. In particular, the energy conservation in the junction reads $\dot{Q}_L + \dot{Q}_R + IV = 0$, and the entropy production rate $\dot{S} = -\dot{Q}_L/T_L - \dot{Q}_R/T_R$ is not negative [1, 22, 33], accordingly to the second law of the thermodynamics [34, 35]. As a consequence, at equal temperatures $T_L = T_R = T$ it follows $IV \geq 0$. Conversely, for $T_L \neq T_R$, the condition $IV < 0$ is possible. For instance, in a thermo-electric system we have $\dot{S} > 0$ provided that $\dot{Q}_{\text{hot}} > 0$ and the efficiency $\eta = -IV/\dot{Q}_{\text{hot}}$ is below the Carnot efficiency, $\eta \leq \eta_C = 1 - T_{\text{cold}}/T_{\text{hot}}$.

Let us consider the charge current I from Eq. 1 and assume EH symmetric quasiparticle DoS $N_\alpha(E) = N_\alpha(-E)$, to satisfy the relation $I(V) = -I(-V)$. Essentially, the condition on the existence of a thermo-electric power $\dot{W} > 0$ can be expressed as the possibility of having an absolute negative conductance (ANC), $I(V)/V < 0$, under a thermal bias. Thanks to EH symmetry, we focus on $V > 0$ and ask whether we can have $I(V) < 0$ in the presence of a temperature difference in the leads. To this purpose, we rewrite, with simple manipulations, the charge current I of Eqs. 1 as

$$I(V) = \frac{G_T}{e} \int_0^\infty dE N_L(E) f_L(E) [N_R(E_+) - N_R(E_-)] + \frac{G_T}{e} \int_0^\infty dE N_L(E) [N_R(E_-) f_R(E_-) - N_R(E_+) f_R(E_+)] \quad (2)$$

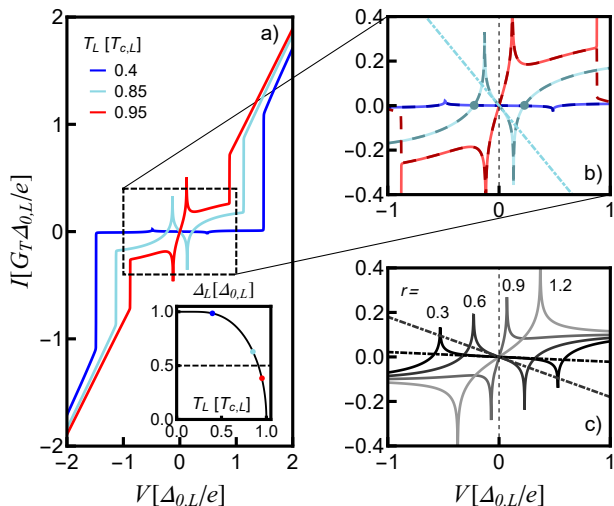


FIG. 1. (color online). **a)** Quasiparticle current-voltage characteristic of a thermally biased tunnel junction between two superconductors (SIS junction) for $T_R = 0.01T_{c,L}$, $r = 0.5$ and different values of $T_L > T_R$. The curves displays an absolute negative conductance (ANC) and hence a thermoelectric power $\dot{W} = -IV > 0$ at small voltage bias provided that $\Delta_L(T_L) > \Delta_{0,R}$. Inset: temperature dependence of the superconducting gap Δ_L . The colored points mark the values of $\Delta_L(T_L)$ for the curves displayed in the panel a). The horizontal dashed line intercepts the Δ_L curve at the point for which the condition $\Delta_L(T_L) = \Delta_R(T_R)$ holds, which is the maximum temperature for the existence of the ANC in panels a) and b). **b)** Enlargement of the subgap transport in panel a) (dashed rectangle). Dashed curves give the first term of Eq. 2. The light-blue dots give the values of the Seebeck voltage V_S . **c)** Subgap IV characteristics for $T_L = 0.7T_{c,L}$, $T_R = 0.01T_{c,L}$, and different values of r . The slopes of the dash-dotted lines in panels b) and c) give the values of the ANC at $V \approx 0$, as expressed by Eq. 4.

where $E_{\pm} = E \pm eV$. If N_L is a gapped function (with gap Δ_L), that is $N_L \approx 0$ for $|E| < \Delta_L$, the second term in Eq. 2 is negligible when $eV, k_B T_R \ll \Delta_L$, due to the exponential damping of the cold distribution f_R . Moreover, for $k_B T_L \lesssim \Delta_L$, the integrand function in the first term of Eq. 2 is finite, owing to the presence of the hot distribution f_L , and negative when $N_R(E)$ is a monotonically decreasing function for $E > \Delta_L - eV$. In conclusion, even with EH symmetric DoS, the presence of the gap and the monotonically decreasing function may generate an ANC, and hence thermoelectricity $\dot{W} = -IV > 0$.

We consider now a prototype system with nearly perfect EH symmetric DoS, namely a tunnel junction between two Bardeen-Cooper-Schrieffer (BCS [36]) superconductors (SIS junction). In this case, the DoS read $N_{\alpha} = \theta(|E| - \Delta_{\alpha})|E|/\sqrt{E^2 - \Delta_{\alpha}^2}$ [37], where $\Delta_{\alpha}(T_{\alpha})$ are the superconducting order parameters. In particular, each function $\Delta_{\alpha}(T_{\alpha})$ is maximum at $T_{\alpha} = 0$ (where it yields $\Delta_{0,\alpha}$), it decreases monotonically with T_{α} and it becomes zero when the temperature approaches the crit-

ical value $T_{c,\alpha}$, following a universal relation, obtained through a self-consistent calculation [29] (see the inset of Fig.1a). Within this model, the standard BCS relation $\Delta_{0,\alpha} = 1.764k_B T_{c,\alpha}$ holds. Hereafter, we will consider the case where the two gaps at zero-temperature differ so we define an asymmetry parameter $r = \Delta_{0,R}/\Delta_{0,L} = T_{c,R}/T_{c,L}$. For simplicity, in this work we completely disregard the Josephson effect occurring in SIS junctions. This condition can be achieved experimentally either by considering a junction with a strongly oxidized barrier or by applying an external in-plane magnetic field.

Consider now Eq. 2 for a SIS junction. As discussed above, for $k_B T_R \ll \Delta_L(T_L)$ the second term is negligible and $I(V)$ is given by the first contribution. To have an ANC, two conditions must apply: i) the hot temperature T_L must be of the order of the gap, $k_B T_L \lesssim \Delta_L(T_L)$, due to the presence of $f_L(E)$ (but necessarily smaller than $T_{c,L}$ for the superconductivity to survive), ii) the term in the square bracket must be negative. Since the BCS DoS $N_R(E)$ is monotonically decreasing only for $E > \Delta_R(T_R)$, the two conditions require

$$\Delta_L(T_L) - \Delta_R(T_R) > 0. \quad (3)$$

Given that $\Delta_L(T_L)$ is a monotonically decreasing function, the conditions are met only if the hot superconductor has the larger gap. Thus, a necessary condition for the ANC is $r < 1$ when $T_L > T_R$ [38].

Figure 1a displays the IV characteristics for $r = 0.5$, $T_R = 0.01T_{c,L}$ and different values of $T_L > T_R$. The evolution is linear $I \simeq G_T V$ at large bias $eV > \Delta_L(T_L) + \Delta_R(T_R)$ and strongly nonlinear within the gap, i.e. for $eV < \Delta_L(T_L) + \Delta_R(T_R)$. Figure 1b gives an enlarged view of the subgap transport displayed in Fig. 1a (dashed rectangle). Within the gap, the curves display characteristic peaks at $eV_{\text{peak}} = \pm|\Delta_L(T_L) - \Delta_R(T_R)| \sim \pm|\Delta_L(T_L) - \Delta_{0,R}|$, due to the matching of the BCS singularities in the DoSs, which creates regions of negative-differential conductance [29, 30]. More interestingly, the curves display also a significant ANC, and hence thermoelectricity, for intermediate values of T_L . Furthermore, the thermoelectric effect is negligible if $\Delta T = T_L - T_R$ is too low and it is absent when $\Delta_L(T_L) < \Delta_R(T_R)$. The contributions due to the first term of Eq. 2 are displayed with dashed lines in Fig. 1b. As argued above, they yield a good approximation for $eV < \Delta_L$, but they are inaccurate at large bias. The dependence of the IV characteristics on r is visualized in Fig. 1c for $T_L = 0.7T_{c,L} > T_R = 0.01T_{c,L}$. In particular, the ANC is present only when $\Delta_{0,R} < \Delta_L(T_L) \sim 0.83\Delta_{0,L}$, namely for $r \lesssim 0.83$.

For $V \sim 0$, the IV characteristic is approximately linear and, by using the first term of Eq. 2, we can derive

an expression for the negative conductance, namely

$$G_0 = \lim_{V \rightarrow 0} \frac{I(V)}{V} = -2G_T \Delta_{0,R}^2 \int_{\Delta_L(T_L)}^{\infty} dE \frac{N_L(E) f_L(E)}{(E^2 - \Delta_{0,R}^2)^{3/2}}, \quad (4)$$

valid for $T_R \ll T_{c,R}$ and $\Delta_L(T_L) > \Delta_{0,R}$. This negative slope is shown in Fig. 1b-c for some curves with dotted-dashed lines, which well represent the low-bias behaviour.

We stress that the existence of the ANC in a thermally biased SIS junction seems not discussed in the literature to the best of our knowledge, despite the central role of superconducting junctions in the field of coherent caloritronics [8]. This is not totally surprising, since the ANC can be observed only for $r \neq 1$ and higher temperature of the larger gap superconducting electrode $T_L \sim T_{c,L}$. However, the features of this effect are reminiscent of the ANC predicted [39] and observed in experiments on nonequilibrium superconductivity, with particles injection [40–42] or microwave irradiation [43].

Thermoelectric figures of merit. Now we consider some relevant figures of merit to characterize the thermoelectric effect. Due to the nonlinear nature of the effect, we cannot rely on the standard figures of merit for the linear thermo-electric effect such as the Seebeck (\mathcal{S}) or the Peltier (\mathcal{P}) coefficients [1, 44]. Yet, in the nonlinear regime we can define the Seebeck voltage V_S which corresponds to the voltage developed by the thermal bias ΔT at open circuit (in the linear regime $V_S = \mathcal{S}\Delta T$). Consider, for instance, the light blue curve in Fig. 1b, where there is thermoelectricity $\dot{W} > 0$. Clearly, the curve crosses the x-axis in $V = 0$, as required by EH symmetry. In the presence of the thermo-electric effect, the junction has an ANC at low voltage ($I/V < 0$) and an Ohmic behaviour at large voltage ($I/V \sim G_T > 0$). Hence, there are at least two finite values $V = \pm V_S \neq 0$ where the current is zero (see marked points in Fig. 1b).

Figure 2a displays the absolute value of the Seebeck voltage $|V_S|$ as a function of r for $T_R = 0.01T_{c,R}$ and some values of $T_L > T_R$ (solid lines). The curves show some characteristic features: i) for a given T_L , V_S decreases monotonically with r and it is zero when r is larger than some critical value (depending on T_L), ii) for a given r , V_S decreases when the temperature T_L , that is proportional to the temperature difference ΔT , is increased. The latter property is peculiar of the nonlinear nature of the discussed thermoelectric effect. Usually the Seebeck voltage is proportional to the thermal gradient in the linear regime, but here, in the nonlinear regime, this is violated. These features can be qualitatively understood by comparing V_S with the matching peak value $V_{\text{peak}} = [\Delta_L(T_L) - \Delta_R(T_R)]/e$ (displayed in Fig. 2a with dashed lines). In fact, the magnitude of V_S is correlated to V_{peak} , namely the order relation $|V_S| \geq V_{\text{peak}}$ holds when there is thermoelectricity (see Fig. 1b,c). By definition, for a given T_L , V_{peak} decreases almost linearly

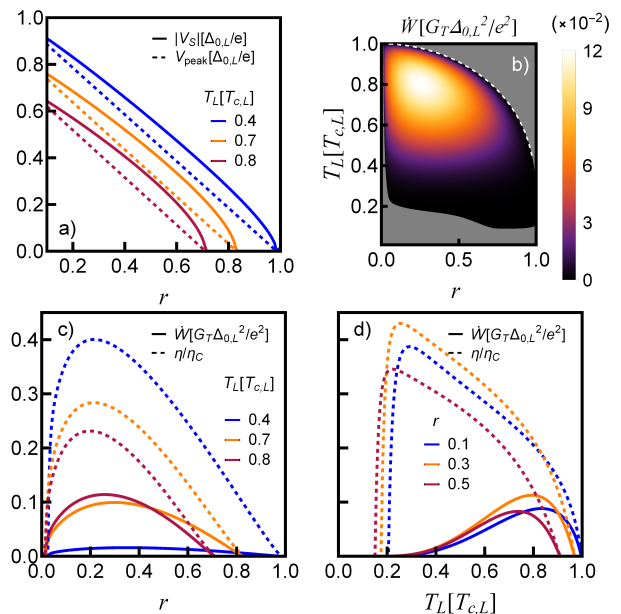


FIG. 2. (color online). Thermoelectric figures of merit for a SIS junction. **a)** Seebeck voltage as a function of r for $T_R = 0.01T_{c,L}$ and some values of $T_{c,L}$ (solid). The voltage corresponding to the singularity matching peak is displayed for a comparison (dashed). **b)** Density plot of the thermoelectric power $\dot{W} = -IV$ vs r and T_L for $T_R = 0.01T_{c,L}$. The gray area denotes the region where the thermoelectric effect is absent, i.e. the junction is dissipative $\dot{W} < 0$. The white dashed curves display the equation $\Delta_L(T_L) = \Delta_{0,R}$. **c),d)** Cuts of Fig. 2b for some particular values of r and T_L , respectively. The correspondent thermoelectric efficiency $\eta = \dot{W}/\dot{Q}_L$ (scaled to the Carnot efficiency $\eta_C = 1 - T_R/T_L$) is plotted with dashed lines.

with r , i.e. $eV_{\text{peak}}/\Delta_{0,L} \sim \Delta_L(T_L)/\Delta_{0,L} - r$. This explains also the temperature evolution, since $\Delta_L(T_L)$ is a monotonically decreasing function. In particular, when r is larger than a critical value depending on T_L , i.e. $r \gtrsim \Delta_{0,R}/\Delta_L(T_L)$, V_S goes to zero since Eq. 3 is violated, i.e. there is no thermoelectricity.

Now, we consider the thermoelectric power $\dot{W} = -IV$. For simplicity, we evaluate this quantity at V_{peak} , which gives us a good estimate of the case of maximum power since $-I(V_{\text{peak}})V_{\text{peak}} \sim \max_V(-IV)$. Figure 2b displays the density plot of \dot{W} as a function of r and T_L for $T_R = 0.01T_{c,L}$. The thermoelectric power is absent if the temperature gradient is too small $T_L - T_R \sim T_L \leq 0.1T_{c,L}$ irrespectively of r . Furthermore, it is zero when $\Delta_L(T_L) < \Delta_{0,R}$ (the dashed white line in Fig. 2b displays the curve $\Delta_L(T_L) = \Delta_{0,R}$). As a consequence, for $T_R = 0.01T_{c,L}$, the maximum value of \dot{W} is obtained at $r \sim 0.25$ and $T_L = 0.8T_{c,L}$ and it yields $\dot{W}_{\text{max}} \sim 0.11 G_T \Delta_{0,L}^2 / e^2$.

For a better characterization, we consider cuts of Fig. 2b (solid lines), for specific values of T_L (see Fig. 2c) and r (see Fig. 2d). In both the panels, we add the cor-

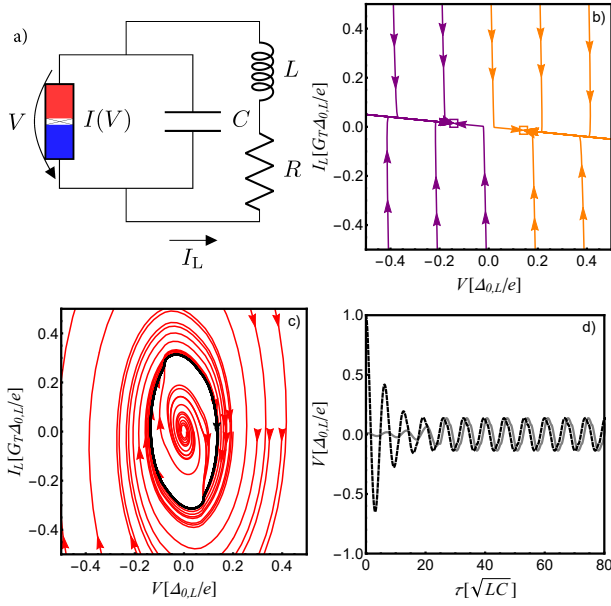


FIG. 3. (color online). **a**) Circuit scheme of the device: the junction is modeled as a parallel circuit composed of a capacitance C and a nonlinear element with characteristic $I(V)$. The external circuit is a generic RL circuit. **b**) Phase portrait for $R = 10G_T^{-1}$. Depending on the initial conditions, the trajectories ends up either in $(V_+, I(V_+))$ (orange-edge rectangle) or $(V_-, I(V_-))$ (purple-edge rectangle), where $V_{\pm} = \pm\tilde{V}$ and \tilde{V} is a non-trivial solution of $RI(\tilde{V}) + \tilde{V} = 0$. **c**) Phase portrait for $R = 0.1G_T^{-1}$. All the trajectories ends up in a limit cycle (black curve). **d**) Time evolution of the voltage across the junction V for some specific initial conditions. After a transient period, the evolution is periodic, as expected from the phase portrait shown in panel c). Parameters are: $G_T^{-1} = 100\Omega$, $L = 100$ pH, $C = 50$ fF, $T_L = 0.7T_{c,L}$, $T_R = 0.01T_{c,L}$, and $r = 0.75$.

respondent thermoelectric efficiency $\eta = \dot{W}/\dot{Q}_L$ (dashed lines), scaled to η_C . Interestingly, the highest efficiency with respect to r is obtained almost in correspondence of the maximum power $\eta_{\max} \sim 40\% \eta_C$ (see Fig. 2c). Conversely, the best condition for η as a function of T_L does not coincide with the condition for the maximum power (see Fig. 2d). This is a common situation of power vs efficiency trade-off. Notably, η is quite high even at the best condition in terms of power $\eta_{\dot{W}_{\max}} = \eta(T_L = 0.8T_{c,L}) \sim 0.22 \eta_C$ (orange line in Fig. 2d).

Applications. Here we sketch two intriguing applications of the thermoelectric effect in the SIS junction: i) a thermal memory, which relies on the existence of a multi-valued Seebeck voltage V_S at a given thermal gradient, ii) a relaxation oscillator [45], thanks to the presence of the ANC in the $I(V)$ characteristic. To discuss both the applications, we consider the junction's dynamics. In particular, we analyze the circuit displayed in Fig. 3a. The junction is modeled as a nonlinear element of characteristic $I(V)$ and capacitance C , in parallel with the

series of L and R , which are the inductance and the resistance of the external circuit connected to the junction, respectively. The nonlinear dynamical system yields

$$\begin{cases} I_L = C\dot{V} + I(V) \\ V = -L\dot{I}_L - RI_L, \end{cases} \quad (5)$$

where I_L is the total current flowing in the circuit and the dot denotes the first derivative with respect to time t . The stationary points are obtained by setting $\dot{I}_L = \dot{V} = 0$ in Eqs. 5 and read $(V(t) = \tilde{V}, I_L(t) = I(\tilde{V}))_2$ where \tilde{V} is a solution of the implicit equation $RI(\tilde{V}) + \tilde{V} = 0$. Since $I(V) = -I(-V)$, the equation has an odd number of solutions and $\tilde{V} = 0$ is always a solution, irrespectively of R . When we apply a temperature gradient and the SIS junction displays thermoelectricity, the conductance G_0 is negative (see Eq. 4), and additional solutions are possible. In particular, this happens when $R > |V_{\text{peak}}/I(V_{\text{peak}})|$, due to the typical shape of the characteristics (see Fig. 1b). In the limit $R \rightarrow \infty$ (open circuit) there are three solutions $\tilde{V} = 0, \pm V_S$ (see Fig. 1b). The stability of these solutions can be inquired with a standard linearization procedure of Eqs. 5 around the stationary points (see Supplemental Material). Here we focus on the case $|G_0|\sqrt{L/C} > 1$, where the solution $\tilde{V} = 0$ is unstable irrespectively of R . This is consistent with realistic parameter values (see the caption of Fig. 3).

Thermoelectric memory. Multiple stable solutions are necessary for memory applications, therefore we consider large values of R . More precisely, for $R > R_0 = |G_0|^{-1}$, there are three stationary solutions: $\tilde{V} = 0$, that is unstable, and $\tilde{V} = V_{\pm}$, which are stable (see Supplemental Material). Figure 3b displays the phase portrait for $R = 10G_T^{-1}$. All the trajectories evolves toward one of the two stationary values at finite voltage $V_{\pm} \sim \pm V_S$, depending on the initial conditions. This kind of memory is volatile, i.e. the system relaxes to $I_L = V = 0$ when the thermal gradient is removed.

Thermoelectric oscillator. Consider now the limit $R \rightarrow 0$, where there is only an unstable stationary solution $\tilde{V} = 0$. Figure 3c displays the phase portrait for $R = 0.1G_T^{-1}$. The plot looks quite different compared to Fig. 3b. In particular, all the trajectories collapse on a close curve in the phase plane, known as the *limit cycle* (black curve). As a consequence, the system displays self-sustained oscillations after a transient dynamics, as better visualized in Fig. 1d for some initial conditions. Namely, the circuit acts as a *thermoelectric relaxation oscillator*, i.e. a system whose oscillations are produced by the presence of a thermal gradient. The period and the shape of the steady-state oscillating signal depend strongly on the features of the $I(V)$ function. For $R \rightarrow 0$, a characteristic time scale for the steady state evolution is $\tau_{\text{per}} = 2\pi\sqrt{LC}$, which is exactly the period of the sinusoidal oscillation in the absence of non-linearity. Strong non-linearities lead to a non-sinusoidal oscillation and to

a longer period of the steady-state dynamics (see Supplemental Material). Therefore, the periodic signal has a frequency $\nu = 1/\tau_{\text{per}}$ in the range 10-100 GHz for typical parameter values.

Conclusions. In summary, we discussed a thermoelectric effect occurring in systems with EH symmetry in transport beyond the linear regime. For a two-terminals tunneling system, characterized by a energy and spin independent transmission matrix, two sufficient conditions are required for thermoelectricity: i) one electrode has a gapped DoS, ii) the other electrode has a locally monotonically decreasing DoS. In particular, we investigated a prototype system which satisfies the previous requests: a tunnel junctions between two unequal superconductors. We displayed the relevant figures of merit and discussed two intriguing applications, namely a volatile thermoelectric memory and a thermo-electric relaxation oscillator. This work can represent a promising first step in the exploration of thermo-electric effects of alternative origin.

We acknowledge the Horizon research and innovation programme under grant agreement No. 800923 (SUPERTEC) for partial financial support. A.B. acknowledges the CNR-CONICET cooperation program Energy conversion in quantum nanoscale hybrid devices.

* giampiero.marchegiani@nano.cnr.it

† alessandro.braggio@nano.cnr.it

‡ francesco.giazotto@sns.it

- [1] G. Benenti, G. Casati, K. Saito, and R. Whitney, *Phys. Rep.* **694**, 1 (2017).
- [2] Y. Dubi and M. Di Ventra, *Rev. Mod. Phys.* **83**, 131 (2011).
- [3] R. Kosloff, *Entropy* **15**, 2100 (2013).
- [4] U. Seifert, *Rep. Prog. Phys.* **75**, 126001 (2012).
- [5] J. T. Muhonen, M. Meschke, and J. P. Pekola, *Rep. Prog. Phys.* **75**, 046501 (2012).
- [6] M. Campisi, P. Hänggi, and P. Talkner, *Rev. Mod. Phys.* **83**, 771 (2011).
- [7] F. Giazotto, T. T. Heikkilä, A. Luukanen, A. M. Savin, and J. P. Pekola, *Rev. Mod. Phys.* **78**, 217 (2006).
- [8] A. Fornieri and F. Giazotto, *Nat. Nanotechnol.* **12**, 944 (2017).
- [9] N. Brunner, N. Linden, S. Popescu, and P. Skrzypczyk, *Phys. Rev. E* **85**, 051117 (2012).
- [10] A. C. Barato and U. Seifert, *Phys. Rev. Lett.* **114**, 158101 (2015).
- [11] M. Polettni, G. Verley, and M. Esposito, *Phys. Rev. Lett.* **114**, 050601 (2015).
- [12] G. Verley, M. Esposito, T. Willaert, and C. V. den Broeck, *Nat. Commun.* **5**, 4721 (2014).
- [13] M. Carrega, M. Sassetti, and U. Weiss, *Phys. Rev. A* **99**, 062111 (2019).
- [14] P. Pietzonka and U. Seifert, *Phys. Rev. Lett.* **120**, 190602 (2018).
- [15] S. K. Manikandan, L. Dabelow, R. Eichhorn, and S. Krishnamurthy, *Phys. Rev. Lett.* **122**, 140601 (2019).
- [16] N. R. Claughton and C. J. Lambert, *Phys. Rev. B* **53**, 6605 (1996).
- [17] K. Brandner, K. Saito, and U. Seifert, *Phys. Rev. Lett.* **110**, 070603 (2013).
- [18] B. Sothmann, R. Sánchez, and A. N. Jordan, *Nanotechnology* **26**, 032001 (2014).
- [19] A. Ozaeta, P. Virtanen, F. S. Bergeret, and T. T. Heikkilä, *Phys. Rev. Lett.* **112**, 057001 (2014).
- [20] M. Esposito, K. Lindenberg, and C. V. den Broeck, *EPL* **85**, 60010 (2009).
- [21] D. Sánchez and L. Serra, *Phys. Rev. B* **84**, 201307 (2011).
- [22] R. S. Whitney, *Phys. Rev. B* **87**, 115404 (2013).
- [23] R. S. Whitney, *Phys. Rev. Lett.* **112**, 130601 (2014).
- [24] F. Giazotto, T. T. Heikkilä, and F. S. Bergeret, *Phys. Rev. Lett.* **114**, 067001 (2015).
- [25] F. Ronetti, L. Vannucci, G. Dolcetto, M. Carrega, and M. Sassetti, *Phys. Rev. B* **93**, 165414 (2016).
- [26] F. Giazotto, J. W. A. Robinson, J. S. Moodera, and F. S. Bergeret, *Appl. Phys. Lett.* **105**, 062602 (2014).
- [27] G. Marchegiani, P. Virtanen, F. Giazotto, and M. Campisi, *Phys. Rev. Applied* **6**, 054014 (2016).
- [28] I. Giaever and K. Megerle, *Phys. Rev.* **122**, 1101 (1961).
- [29] M. Tinkham, *Introduction to superconductivity* (Dover Publications, 2004).
- [30] A. Barone and G. Paternò, *Physics and applications of the Josephson effect* (Wiley, 1982).
- [31] G. D. Mahan, *Many-Particle Physics* (Kluwer Academic/Plenum Publishers, New York, 2000).
- [32] Note that $I_R = -I_L$ due to charge conservation.
- [33] K. Yamamoto and N. Hatano, *Phys. Rev. E* **92**, 042165 (2015).
- [34] I. Prigogine, *Introduction to Thermodynamics of Irreversible Processes* (Thomas, Springfield, 1955).
- [35] S. R. de Groot and P. Mazur, *Non-Equilibrium Thermodynamics* (North-Holland, Amsterdam, 1962).
- [36] J. Bardeen, L. N. Cooper, and J. R. Schrieffer, *Phys. Rev.* **108**, 1175 (1957).
- [37] Realistic junctions displays a small but finite sub-gap transport, due to the finite lifetime of the quasiparticle states. The Dos is typically described in terms of a phenomenological parameter Γ [46], and reads $N_\alpha = |\text{Re}[(E + i\Gamma_\alpha)/\sqrt{(E + i\Gamma_\alpha)^2 - \Delta_\alpha^2}]|$. Typical values are in the range $10^{-5} - 10^{-2}\Delta_0$. In all the calculations we set $\Gamma_\alpha = 10^{-4}\Delta_{0,\alpha}$.
- [38] Clearly, by appropriately inverting the temperature gradient, i.e. $T_R > T_L$, the proper conditions are met for $r > 1$.
- [39] A. G. Aronov and B. Z. Spivak, *JETP Lett.* **22**, 101 (1975).
- [40] M. E. Gershenzon and M. I. Falei, *JETP Lett.* **44**, 682 (1986).
- [41] M. E. Gershenzon and M. I. Falei, *Sov. Phys. JETP* **67**, 389 (1988).
- [42] J. G. Gijsbertsen and J. Flokstra, *J. Appl. Phys.* **80**, 3923 (1996).
- [43] J. Nagel, D. Speer, T. Gaber, A. Sterck, R. Eichhorn, P. Reimann, K. Ilin, M. Siegel, D. Koelle, and R. Kleiner, *Phys. Rev. Lett.* **100**, 217001 (2008).
- [44] G. D. Mahan, *J. Appl. Phys.* **65**, 1578 (1989).
- [45] P. Horowitz and W. Hill, *The Art of Electronics* (Cambridge University Press, 2015).
- [46] R. C. Dynes, J. P. Garno, G. B. Hertel, and T. P. Orlando, *Phys. Rev. Lett.* **53**, 2437 (1984).

Supplemental Material: Nonlinear thermoelectricity with particle-hole symmetry in transport

G. Marchegiani,^{1,*} A. Braggio,^{1,†} and F. Giazotto^{1,‡}

¹*NEST Istituto Nanoscienze-CNR and Scuola Normale Superiore, I-56127 Pisa, Italy*

(Dated: May 17, 2022)

*Electronic address: giampiero.marchegiani@nano.cnr.it

†Electronic address: alessandro.braggio@nano.cnr.it

‡Electronic address: francesco.giazotto@sns.it

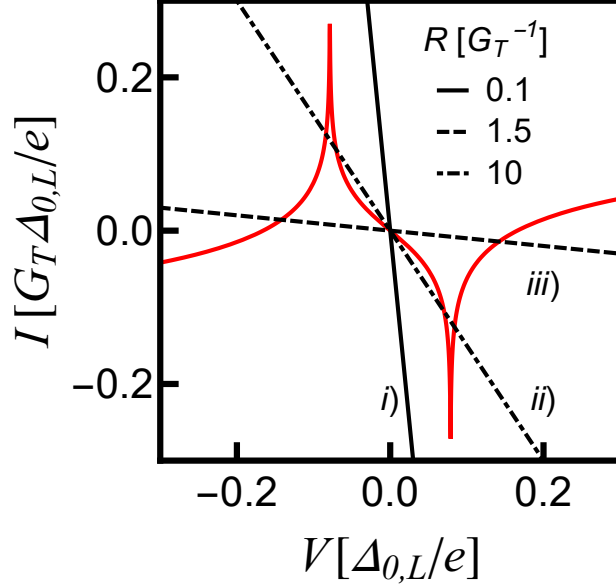


FIG. 1: (color online). Graphical solution of Eq. 2. The solutions are given by the crossings of the $I(V)$ characteristic (red curve) and the load line $-V/R$ (black lines). Depending on the slope of the load line, we can have up to 5 different solutions. In the main text, we discussed case i) (1 solution) and case iii) (3 solutions) for the relaxation oscillator and the thermoelectric memory applications, respectively.

I. STABILITY ANALYSIS

We start by rewriting the system of Eqs.5 of the main text in the following way:

$$\begin{cases} \dot{V} = \frac{1}{C}[-I(V) + I_L] \\ \dot{I}_L = -\frac{1}{L}V - \frac{R}{L}I_L. \end{cases} \quad (1)$$

The latter is a system of two nonlinear differential equations of the first order. As discussed in the main text, the stationary points are obtained by setting $\dot{I}_L = \dot{V} = 0$. Hence, the first of Eqs. 1 requires $I_L = I(V)$, which inserted in the second of Eqs. 1 produces the implicit equation:

$$I(V) + \frac{V}{R} = 0. \quad (2)$$

Due to the particle-hole symmetry of the transport, $I(V = 0) = 0$ and hence $V = 0$ is a solution of Eq. 2 irrespectively of R . Moreover, in the absence of the thermoelectric effect, the trivial solution is the unique solution since $R > 0$ and $I(V)$ and V shares the same sign,

i.e $IV \geq 0$. In the presence of the thermoelectric effect we have $IV < 0$ for some voltage biases and Eq. 2 can have additional solutions.

In particular, the set of solutions of Eq. 2 are geometrically given by the crossings of the load line $I = -V/R$ and the $I(V)$ characteristic of the junction. Figure 1 gives the graphical solution of Eq. 2 for the temperature bias considered in the numerical calculation in the main text, i.e. $T_L = 0.7T_{c,L}$, $T_R = 0.01T_{c,L}$. The number of solutions is obtained by counting the crossings and can be classified as follows

$$\begin{cases} i) R < |V_{\text{peak}}/I(V_{\text{peak}})| & 1 \text{ solution} \\ ii) |G_0^{-1}| > R > |V_{\text{peak}}/I(V_{\text{peak}})| & 5 \text{ solutions} \\ iii) R > |G_0^{-1}| & 3 \text{ solutions} \end{cases} \quad (3)$$

In the main text, we discussed case i) and case iii) for the relaxation oscillator and the memory application, respectively. For simplicity, we discuss the stability of the stationary points with a linearization procedure [1]. In particular, upon linearizing the system of Eqs. 1 around the generic solution $V = \tilde{V}$ of Eq. 2, we get

$$\frac{d}{dt} \begin{pmatrix} v \\ i_L \end{pmatrix} = A \begin{pmatrix} v \\ i_L \end{pmatrix} = \begin{pmatrix} -G(\tilde{V})/C & 1/C \\ -1/L & -R/L \end{pmatrix} \begin{pmatrix} v \\ i_L \end{pmatrix} \quad (4)$$

where $v = V - \tilde{V}$, $i_L = I_L - I(\tilde{V})$ and $G(\tilde{V}) = dI/dV|_{V=\tilde{V}}$. Clearly, $G(\tilde{V} = 0) = G_0$. The solution of the linearized system can be obtained by computing the eigenvalues λ_{\pm} of the 2x2 matrix A of Eqs. 4. They reads:

$$\lambda_{\pm} = \frac{\Sigma}{2} \pm \sqrt{\left(\frac{\Sigma}{2}\right)^2 - D} = 0, \quad (5)$$

where $\Sigma = \text{Tr}[A] = -G(\tilde{V})/C - R/L$ and $D = \text{Det}[A] = (G(\tilde{V})R + 1)/(LC)$ are the trace and the determinant of the A matrix, respectively. The stationary point is stable if the real parts of both the solutions λ_{\pm} are negative [1]. For $D < 0$, we observe that the two solutions of Eq. 5 are reals and they have opposite signs, i.e. the stationary point is unstable. Conversely, for $D > 0$, the signs of the real parts of λ_{\pm} are equal to the sign of Σ . As a consequence, one gets a stable solution when $\Sigma < 0$ and $D > 0$. Moreover, when $D > \Sigma^2/4$, the eigenvalues get also an imaginary component which gives the frequency of oscillation of the overdamped evolution when the system evolves toward the stationary solution.

With respect to our system of Eqs. 4, we note that $G(V) > 0$ implies $\Sigma < 0$ and $D > 0$, hence each stationary point with positive conductance is stable, corresponding to a dissipative behavior. Conversely, the case $G(V) = -|G(V)| < 0$ gives a richer phenomenology. Since $\Sigma < 0$ gives $R > |G(V)|L/C$ and $D > 0$ implies $R < |G(V)|^{-1}$, it is possible to have values of R which give a stable solution only when $|G(V)|\sqrt{L/C} < 1$.

We are now ready to discuss the two different regimes considered in the main text, where we analyzed a situation with $|G(V)|\sqrt{L/C} > 1$, which makes $V = 0$ an unstable solution irrespectively of R .

Thermoelectric memory-case iii). We have three stationary points $V = 0, \tilde{V}_{\pm}$. The solution $V = 0$ is unstable irrespectively of L, C . Indeed $G(\tilde{V} = 0) = -|G_0| < 0$ and the condition $R < |G(V)|^{-1} = |G_0|^{-1}$ is violated, as discussed in the classification of Eqs. 3. Conversely, the two solutions $V = \tilde{V}_{\pm}$ are stable since $G(\tilde{V}_{\pm}) > 0$. Therefore, each trajectory in the phase portrait evolves either toward \tilde{V}_{+} or \tilde{V}_{-} , depending on the initial conditions.

Thermoelectric oscillator-case i). There is a unique stationary point, i.e. the trivial solution $V = 0$, where $G(\tilde{V} = 0) = -|G_0| < 0$. In the numerical calculation of the main text, we consider a set of realistic parameters which satisfy the inequality $|G_0|\sqrt{L/C} > 1$. As a consequence, the stationary point is unstable irrespectively of R , giving rise potentially to an oscillatory behavior as we discuss now.

II. EXISTENCE AND UNIQUENESS OF THE LIMIT CYCLE

For simplicity, we focus on the limit $R \rightarrow 0$ and we write a second order differential equation for V by combining the two equations of the system of Eqs. 1

$$\ddot{V} + \sqrt{\frac{L}{C}}G(V)\dot{V} + V = 0, \quad (6)$$

where the dot gives the time derivative with respect to the dimensionless time $\tau = t/\sqrt{LC}$. Note that $G(V) = dI(V)/dV$ is an even function of V since $I(V)$ is a odd function. As a consequence, Eq. 6 is of the Liénard type $\ddot{x} + f(x)\dot{x} + g(x) = 0$, where $f(x)$ is an even function and $g(x)$ is an odd function.

For $g(x) = x$, as in our case, a generalization of the Levinson-Smith theorem states that a dynamical system of the Liénard type displays a unique stable cycle limit under the following assumptions [2, 3]:

- exists $x_0 > 0$ such that $f(x) < 0$ for $|x| < x_0$
- either $f(x) > 0$ in (x_0, ∞) or $f(x) > 0$ in $(-\infty, -x_0)$
- exists $x_1 > 0$ such that $F(x_1) = F(-x_1) = 0$
- $\lim_{x \rightarrow \pm\infty} F(x) = \pm\infty$

where $F(x)$ is the primitive of $f(x)$.

In our case $f(x) = G(V)$, $F(x) = I(V)$. Note that the last condition is always satisfied, since $I(V) \sim G_{\text{T}}V$ at large V . In the presence of a thermoelectric effect, we have that $G(V) < 0$ for $|V| < V_{\text{peak}}$ and positive otherwise. As a consequence, all the remaining assumptions are satisfied with $x_0 = V_{\text{peak}}$ and $x_1 = |V_{\text{S}}|$.

In general, the properties of the steady state oscillation, i.e. the period and the shape of the signal, depend on the details of the nonlinear term $G(V)$. This can be understood by looking at the standard examples of negative resistance oscillators, such as the Van Der Pol oscillator or the piecewise linear oscillator [1, 4]. Two limits are typically discussed:

Small non-linearity. As a first approximation, one can solve Eq. 6 by neglecting the second term when the non-linear term $|G(V)\sqrt{L/C}|$ is small. The solution of the linear equation is a sinusoidal oscillation $V(t) = \mathcal{A}\sin(\omega t)$ with characteristic frequency $\nu = \omega/(2\pi) = 1/(2\pi\sqrt{LC})$. Note that, unlike a proper linear system, the amplitude of the oscillation \mathcal{A} is fixed by the non-linearity of the problem, since the limit cycle is unique.

Large non-linearity. The steady-state is characterized by a slow-fast dynamics. The shape of the signal depends strongly on the non-linear term and the period can be computed, in simple cases, through a perturbative approach. Typically the frequency scales with the strength of the non-linear term and hence it is reduced with respect to the almost-linear situation. This is well known and described for standard systems like the Van Der Pol oscillator [4].

-
- [1] S. Strogatz, *Nonlinear Dynamics and Chaos: With Applications to Physics, Biology, Chemistry, and Engineering*, Studies in Nonlinearity (Avalon Publishing, 2014).
- [2] G. Sansone, Ann. Mat. Pura Appl **28**, 153 (1949).
- [3] M. Sabatini and G. Villari, Matematiche **LXV(Fasc. II)**, 201 (2010).

- [4] J. Stoker, *Nonlinear Vibrations in Mechanical and Electrical Systems* (Interscience Publishers, 1950).